VIP Ionic Liquids

DOI: 10.1002/anie.201302712

From Short-Range to Long-Range Intermolecular NOEs in Ionic Liquids: Frequency Does Matter**

*Sonja Gabl, Othmar Steinhauser, and Hermann Weingärtner**

The nuclear Overhauser effect (NOE) is widely used for studying local structures in liquids and solutions.[1] The NOE reflects cross-relaxation between two nuclear spins, I and S, because of magnetization transfer through coupling of their magnetic dipole moments. With increasing internuclear distance r the cross-relaxation rate σ_{IS} decays as $1/r^6$. Thus, a NOE is only achieved, if r is less than 4–5 Å.[2]

While derived for spins in the same molecule, a rule like this is also applied to intermolecular cross-relaxation, implying that the NOE essentially captures molecules in the innermost coordination sphere of the relaxing particle. To generate a notable probability for magnetization transfer the life time of these configurations has to be at least of the order of the inverse Larmor frequency $1/\omega_I$ of the relaxing spin I.[2] In ^{1}H NMR spectroscopy this time is typically of the order of 0.5 ns. The specificity of NOE spectroscopy to local interactions prospects intriguing applications. In the present work we focus on NOE studies of local ion configurations in ionic liquids (ILs),[3] but our results are prototypical for many other classes of liquids as well.

As a representative example, we consider results on the ^{1}H-^{19}F NOE in 1-butyl-3-methylimidazolium tetrafluoroborate (**1**) by Giernoth's research group,[3a] which appear to indicate the existence of cation–anion pairs with life times on the nanosecond time scale. After a long-standing debate about the definition, existence (or not), and life time of ion pairs in neat ILs,[4] there is now consensus that in **1** (see Scheme 1) and similar ILs long-lived pairs do not exist. Otherwise, ILs would, for example, reveal a distinct ion pair mode in the dielectric relaxation spectrum, which for **1**[5] and similar ILs has never been observed in experiments and simulations.[6]

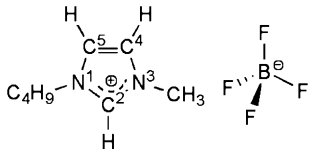

Scheme 1. 1-Butyl-3-methylimidazolium tetrafluoroborate (**1**).

[*] Prof. Dr. H. Weingärtner
Department of Physical Chemistry II
Ruhr-University of Bochum, 44780 Bochum (Germany)
E-mail: hermann.weingaertner@rub.de
Mag. S. Gabl, Prof. Dr. O. Steinhauser
Department of Computational Biological Chemistry
University of Vienna, 1090 Vienna (Austria)

[**] This work is supported by the Cluster of Excellence RESOLV (EXC 1069) funded by the Deutsche Forschungsgemeinschaft. NOE = nuclear Overhauser effect.

The situation closely resembles that encountered in studies of protein hydration, where protein–water NOEs mimic a strongly retarded dynamics of hydration water relative to the bulk liquid. As shown by Halle's research group this strongly bound water does not withstand the test of other experiments.[7] A properly formulated theory of the intermolecular NOE in protein–water solutions by Halle[8] predicts a protein–water NOE dominated by long-range dipolar couplings to bulk water rather hydration water.

Taken together, these observations give rise to fundamental questions about the mechanisms governing the intermolecular NOE.

The present paper addresses these issues by exploring the consequences of a new theory of the intermolecular NOE[9] for the interpretation of NOE data in liquids in general and ILs in particular. The results for **1**[3a] are particularly suited for such an analysis because the literature offers auxiliary data for modeling the NOE.

The information provided by the cross-relaxation rate σ_{IS} concerns the spectral density function $J(\omega)$, which describes the modulation of the magnetic dipole–dipole interaction between the spins I and S by molecular motions. For ^{1}H-^{19}F heteronuclear NOE spectroscopy in the laboratory (Zeeman) frame σ_{IS} is given by Equation (1),[2]

$$\sigma_{IS} = 0.6J(\omega_I + \omega_S) - 0.1J(\omega_I - \omega_S) \quad (1)$$

where ω_I and ω_S are the Larmor frequencies of the spins I and S. σ_{IS} involves the response at two frequencies, namely the sum frequency $(\omega_I + \omega_S)$ and the difference frequency $(\omega_I - \omega_S)$. The understanding of the NOE is founded in a different behavior of these two terms.

While the frequency dependence of $J(\omega)$ prospects detailed information on the intermolecular structure and dynamics,[10] NOE data are usually acquired at a single frequency. This loss of information makes their interpretation highly model-dependent. Most NOE studies resort to a short-range spectral density function of the form given in Equation (2),[2]

$$J(\omega) = K_{IS}\frac{1}{r^6}\frac{\tau_c}{1+(\omega\tau_c)^2} \quad (2)$$

which can be theoretically derived under the assumption that during magnetization transfer the internuclear vector $\mathbf{r}$ connecting I and S has a fixed length r (bold quantities denote vectors), as is the case for an intramolecular NOE.[2] τ_c is the tumbling time of the vector $\mathbf{r}$, $K_{IS} = [(\mu_0/4\pi)\hbar\gamma_I\gamma_S]^2$ is the dipolar coupling constant, where γ_I and γ_S are the magnetogyric ratios of the spins, and μ_0 is the permeability of the vacuum. For ^{1}H-^{19}F spin pairs K_{IS} is 5.04×10^{11} Å^6 s^{-2}.

For the intermolecular cross-relaxation NOE this approach neglects the modulation of the vector **r** by translational diffusion of the particles. It is known for a long time from theories of intermolecular spin–lattice relaxation that translational dynamics renders $J(\omega)$ long-range.[11] Here, we reconsider these issues for a spin I in a cation, interacting with N_S spins S in anions. The complete theory and its relation to earlier approaches will be given elsewhere.[9]

Figure 1 illustrates our model for the intermolecular dynamics. The cation–anion distribution is described by the radial pair distribution function $g(R)$, where the vector **R** connects the centers of mass of the ions. The two spins are

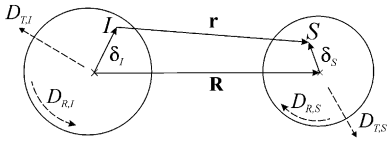

Figure 1. Model for the dynamics governing intermolecular cross-relaxation between the spins I and S.

located at distances δ_I and δ_S from the centers of mass of the ions. The magnetic dipole–dipole interaction between I and S is modulated by translational and rotational motions of the ions. Translational motions modulate the vector **R**, while rotational motions modulate the orientations of the off-center vectors $\boldsymbol{\delta}_I$ and $\boldsymbol{\delta}_S$. Translational diffusion of the ions is described by the relative diffusion coefficient D_T, which is approximated by the sum of the self-diffusion coefficients of the ions, $D_T \cong D_{T,I} + D_{T,S}$. Rotational motions are characterized by the rotational diffusion coefficients $D_{R,I}$ and $D_{R,S}$ of the ions, which are related to the measurable orientational correlation times τ_c by the relation $D_R = (6\tau_c)^{-1}$. The translational and rotational diffusion coefficients are assumed to be spatially uniform.

The time evolution of the magnetic dipole–dipole interaction is obtained by solving the differential equations for rotational and translational diffusion under the boundary conditions given by our model, which leads to a representation of $J(\omega)$ in the reciprocal space with the wave vector **k** instead of **R** as a variable. When approximating $g(R)$ by a uniform distribution of the ions, modeled by a step function ranging from a lower cut-off distance d to infinity, our theory provides an analytical expression for $J(\omega)$. The latter approximation, known as "force-free model",[11c] underlies all theories of intermolecular spin relaxation of interest here. The resulting expression for the spectral density function $J(\omega)$ reads [Eq. (3)],

$$J(\omega) = \rho_S K_{IS} \sum_{l=0}^{\infty} \int_0^{\infty} Q_l(k,\omega) \frac{j_{l+1}(kb)}{b^{l+1}} \left[\frac{j_{l+1}(kb)}{d^{l+1}} - \frac{j_{l+1}(kR)}{R^{l+1}} \right] dk \qquad (3)$$

where ρ_S is the spin density of S. The functions $j_l(x)$ are the spherical Bessel functions of rank l. b is the closest distance of approach between the ions. A molecular dynamics (MD) simulation of $g(R)$[12] yields $b = 3.05$ Å. The distance d defines the onset of the step function. In a self-consistent treatment the choice of $d = 5.28$ Å has to reproduce the spin density of $\rho_S = 1.24 \times 10^4$ Å^{-3} of ^{19}F. The dynamical behavior is captured by the rotational–translational coupling function $Q_l(k,\omega)$ given in Equation (4):

$$Q_l(k,\omega) = C_l \sum_{\lambda=0}^{l} \frac{\delta_I^{2\lambda}}{(2\lambda+1)!} \frac{\delta_S^{2\nu}}{(2\nu+1)!} f_l(k,\omega) \qquad (4)$$

with the abbreviations $C_l = (l+1)\ (l+2)\ (2l+3)\ (2l+1)!/6$ and $\nu = 1-\lambda$. The function [Eq. (5)]

$$f_l(k,\omega) = \frac{k^2 D_T + \lambda(\lambda-1) D_{R,I} + \nu(\nu+1) D_{R,S}}{[k^2 D_T + \lambda(\lambda-1) D_{R,I} + \nu(\nu+1) D_{R,S}]^2 + \omega^2} \qquad (5)$$

represents a combination of the measurable translational and rotational diffusion coefficients. We note that the translational diffusion coefficient is weighted by the square of the wave vector, while the rotational diffusion coefficients are not. For purely translational dynamics only terms with $l = 0$ survive. This limit is achieved, if the spins I and S coincide with the centers of mass of the ions ($\delta_I = \delta_S = 0$). In our calculations convergence was achieved by summing terms up to $l = 6$ to 10.

Based on these equations we have analyzed the ^{1}H-^{19}F heteronuclear NOE of **1** based on three models:

- Model A corresponds to the intermolecular NOE between the proton at carbon C^2 of the imidazolium cation ($\delta_I =$ 1.8 Å) and ^{19}F of the $[BF_4]^-$ anion ($\delta_S = 1.4$ Å).
- Model B considers the NOE between a proton of maximum eccentricity ($\delta_I = 2.8$ Å) in the cation and ^{19}F ($\delta_S =$ 1.4 Å). This choice, albeit exaggerated with regard to the real IL, helps to assess the dependence of the NOE on the spin eccentricity.
- Model C refers to the limiting case of a purely translational mechanism ($\delta_I = \delta_S = 0$).

Table 1 lists the experimental data used in our calculations.[13] While the rotational dynamics of the anions and cations occurs on time scales of 100 and 500 ps, respectively,

Table 1: Dynamical properties used for modeling the spectral density function $J(\omega)$ at 25 °C.[13]

Property	Cation	Anion
D_T [m^2 s^{-1}]	1.40×10^{-11}	1.33×10^{-11}
D_R [s^{-1}]	3.19×10^8	1.41×10^9
τ_c [ps]	522	118

translational motions show a broadly distributed dynamics in the nanosecond regime. The rationale is that a distant pair of spins needs a longer time to randomize the internuclear vector **r** than a pair of neighboring spins. According to the Einstein equation the time τ_{trans} for modulation of the center-to-center vector **R** increases with the mean-square displacement $\langle \mathbf{R}^2 \rangle$ as $\tau_{trans} = \langle \mathbf{R}^2 \rangle / 6 D_T$. With $\langle \mathbf{R}^2 \rangle^{1/2} = 6$ Å, which is a typical distance for the exchange of an anion from the first to the second coordination shell of the cation in **1**, we find $\tau_{trans} = 2.3$ ns.

In simple solvents of low viscosity like aqueous solutions the molecular motions modulating the NOE are of the order of several picoseconds. As a consequence the spectrometer frequencies are substantially below the frequencies of the molecular motions determining the spectral density $J(\omega)$. Then, one approaches the so-called "extreme-narrowing" limit, where $J(0)\cong J(\omega_I-\omega_S)\cong J(\omega_I+\omega_S)$. As a consequence σ_{IS} becomes independent of frequency, and Equation (1) simplifies to $\sigma_{IS}=0.5J(0)$.[2] Much of the literature on the NOE refers to this situation. It is therefore apt to start our analysis by modeling cross-relaxation in this limiting case.

Figure 2 shows the calculated spectral density $J^*(0)$ in the extreme narrowing limit as a function of the center-to-center distance R for the models A to C, supplemented by a sketch of

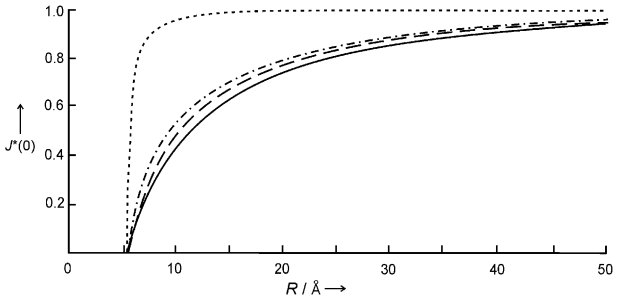

Figure 2. Spectral density function $J^*(0)$ in the extreme-narrowing limit as a function of the center-to-center distance R of the ions for model A (dashed curve), model B (dashed-dotted curve), and model C (solid curve). All curves are normalized to their asymptotic values at large R. The dotted line sketches the R^{-6} dependence as a limiting case.

the short-range R^{-6} dependence. The asterisk of $J^*(0)$ indicates that all curves are normalized by their asymptotic values, which increase with increasing off-center location of the spins. While the R^{-6}-dependent NOE immediately rises to its maximum value (dotted curve), the intermolecular NOEs are long-range. In the translational limit (solid curve) a fit to a distance dependence of the form R^{-n} yields $n=1.1$, which practically implies a $1/R$-dependence, as is also predicted by some early theories of intermolecular spin relaxation of monoatomic liquids.[11] With increasing spin eccentricity, where rotational motions become relevant, the R dependence of the NOE changes only marginally. We find $n=1.17$ for model A and $n=1.27$ for model B, which represents the maximum off-center effect. Thus, in both cases the decay of the spectral density function is still governed by translational dynamics.

Furo's research group has, however, demonstrated[10] that in systems dominated by a broadly distributed translational dynamics this limit is not reached at the typical spectrometer frequencies, even for small molecules in systems of low viscosity. This is even more so, for ILs, the viscosities of which typically exceed those of fluid organic solvents by at least two orders of magnitude (at 25 °C the viscosity of **1** is $\eta=$ 104.9 mPa s[13]). In the latter case the spectral density is shifted downward and "meets" the spectrometer frequency. To elucidate the resulting interplay of the molecular frequencies and the spectrometer frequency, Figure 3 shows the

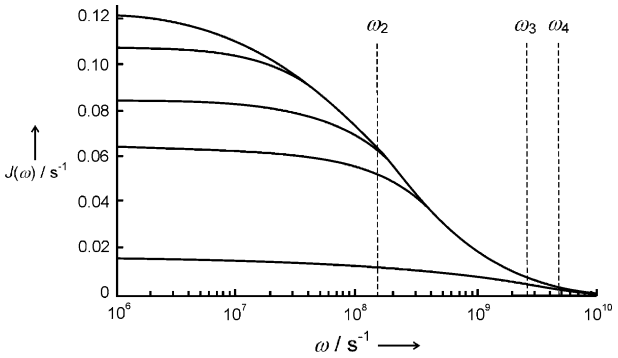

Figure 3. Spectral density function $J(\omega)$ as a function of frequency for model A for selected values of the spatial range, from top to bottom referring to $R=100$, 30, 15, 10, and 6 Å, respectively. The three vertical bars mark the selected spectrometer frequency, $\omega_3=2.51$ GHz ($\nu_3=400$ MHz), the corresponding difference frequency $\omega_2=(\omega_I-\omega_S)=0.15$ GHz, and the sum frequency $\omega_4=(\omega_I+\omega_S)=4.85$ GHz. The ordinate is placed at $\omega_1=1$ MHz, where the extreme-narrowing regime is reached.

complete frequency spectrum $J(\omega)$ for model A for selected values of the spatial range R ranging from 6 to 100 Å. Although widely spread at zero-frequency, the bundle of curves in Figure 3 approaches each other with increasing frequency and the curves finally converge in the asymptotic regime.

It is instructive to consider in more detail results for the spatial dependence of the NOE at four frequencies of particular interest, numbered from low to high frequencies as ω_1 to ω_4. Our calculations are based on a spectrometer frequency of $\omega_3=2.51$ GHz ($\nu=400$ MHz) used in the experiments for **1**. $\omega_1=1$ MHz is representative for the onset of the extreme-narrowing regime. Strikingly, ω_1 is by more than two orders of magnitude below the spectrometer frequencies used in NOE experiments. In other words, in practice the extreme-narrowing limit will never apply for ILs. $\omega_2=(\omega_I-\omega_S)=0.15$ GHz and $\omega_4=(\omega_I+\omega_S)=4.85$ GHz are the corresponding difference and sum frequencies entering into the expression for the cross-relaxation rate given by Equation (1). In Figure 3 the frequencies ω_2 to ω_4 are marked by vertical bars and the ordinate axis is placed at $\omega_1=1$ MHz. The resulting curves for the spatial dependence of the NOE were tentatively fitted to an R^{-n} dependence.

Figure 4 displays the exponents of the R dependence of the NOE at different frequencies. The results reveal a steady transition from long-range behavior of the NOE at low frequencies ($n=1.17$ at $\omega_1=1$ MHz and $n=2.5$ at $\omega_2=(\omega_I-\omega_S)=0.15$ GHz to short-range behavior at high frequencies ($n=7.2$ at $\omega_3=2.5$ GHz and $n=8.2$ at $\omega_4=(\omega_I+\omega_S)=$ 4.85 GHz). Within the limits of the model the latter values are consistent with an R^{-6} dependence of the NOE.

The reason for this transition can be found in the rotational–translational coupling function [Eq. (5)]. For higher frequencies the ω^2 term in the denominator overpowers the contributions at low wave vectors k. Therefore, only the contributions at higher k values contribute significantly while integrating Equation (3). From the reciprocity between the wave vector and real space representations it follows that

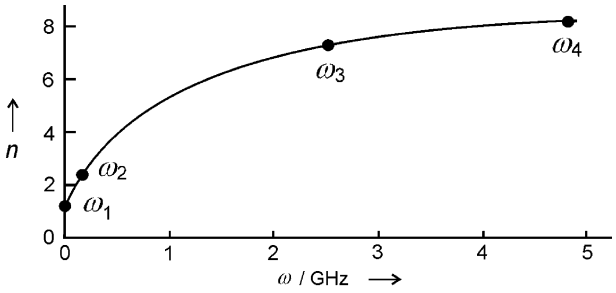

Figure 4. Exponent n characterizing the R^{-n} dependence of the spectral density function $J(\omega)$ for model A as a function of frequency.

the dominance of high k values corresponds to smaller R values, that is, to a shorter range.

However, one should recall that according to Equation (1) the experimental cross-relaxation rate σ_{IS} reflects a linear combination of $J(\omega_I-\omega_S)$ being of intrinsic long-range nature, and $J(\omega_I+\omega_S)$ having short-range character. Since the spectral density function decays monotonically, $J(\omega_I-\omega_S)$ always exceeds $J(\omega_I+\omega_S)$. The latter, however, is weighted six times as large as $J(\omega_I-\omega_S)$, resulting in a complex mixture of long-range and short-range effects. It depends on the particular conditions of the experiments, which part dominates.

In the case of **1** the term at $(\omega_I-\omega_S)$ largely overpowers that at $(\omega_I+\omega_S)$ in Equation (1), so that the measured cross-relaxation rate essentially reflects long-range behavior, if taken literally with an exponent of $n\cong2.5$. Thus, the NOE extends far beyond the first coordination sphere of the cation. Replacing the step function for the ion distribution by a more realistic pair distribution function $g(R)$, for example taken from MD simulations, may soften this long-range behavior. However, the redistribution of the ions into distinct layers essentially concerns interactions up to the second layer, whereas beyond this distance the step function is a good approximation. We therefore only expect minor changes in the R dependence of the NOE.

Taken together our analysis leads to the following conclusions:

- The spatial range captured by the NOE monotonously increases from high to low frequency, indicating a transition from R^{-6}-type short-range behavior to R^{-1}-type long-range behavior. Thus, the two contributions to the heteronuclear NOE at the frequencies $(\omega_I-\omega_S)$ and $(\omega_I+\omega_S)$ display a different R dependence.
- Under the conditions of the study of IL **1**,[7] and presumably for studies of other ILs as well, the contribution at the frequency $(\omega_I-\omega_S)$ largely overpowers that at $(\omega_I+\omega_S)$, resulting in a long-range NOE. Thus, the NOE says little about ions in direct contact, but captures spins far beyond the first coordination layer. Site-specific NOE measurements may therefore reflect the mean orientation of the ions over long distances rather than the local structure of distinct ion aggregates.
- A similar behavior is expected for the homonuclear ^{1}H-^{1}H NOE ($\omega_I=\omega_S$), for example probed in the study of cation–cation interactions in **1** by Mele et al.,[3c] where Equation (1) transcribes into the relation $\sigma_{II}=0.6J(2\omega)-0.1J(0)$. There the two frequencies are even more distant.
- The molecular-level cross-relaxation essentially reflects processes associated with translational motions of the ions. Rotational dynamics of the ions play a marginal role.

We conclude with some final remarks about the consequences of our findings for NOE studies in general:

- In the case of translational motions the broadly distributed dynamics can shift the spectral density to frequencies far below the spectrometer frequencies used in NOE experiments, so that data evaluations based on the extreme-narrowing situation are meaningless. According to the work by Furo and co-workers,[10] this result, pinpointed here for viscous ILs, applies even to systems of comparatively low viscosity.
- Accounting for differences in the model and technical methods, our conclusions are fully consistent with the results of some earlier theories of intermolecular spin relaxation,[11] and notably with theoretical work by Halle.[8] Our results go, however, beyond these studies because, as a striking feature, we observe the spatial range of the NOE to vary with frequency.
- The consistency of conclusions obtained for largely different systems such as ILs and protein solutions suggests that NOEs in many other liquids behave in an analogous fashion.

Received: April 2, 2013
Published online: June 17, 2013

Keywords: ionic liquids · molecular dynamics · NMR spectroscopy · nuclear Overhauser effect

[1] a) H. P. Mo, T. C. Pochapski, *Prog. Nucl. Magn. Reson. Spectrosc.* **1997**, *30*, 1–38; b) J. T. Gerig, *Annu. Rep. NMR Spectrosc.* **2008**, *64*, 21–76.
[2] D. Neuhaus, M. P. Williamson, *The Nuclear Overhauser Effect in Structural and Conformational Analysis*, 2nd ed., Wiley-VCH, Weinheim, **2000**.
[3] a) Y. Lingscheid, S. Arenz, R. Giernoth, *ChemPhysChem* **2012**, *13*, 261–266; b) D. Bankmann, R. Giernoth, *Prog. Nucl. Magn. Reson. Spectrosc.* **2007**, *51*, 63–90; c) A. Mele, G. Romanò, M. Giannone, E. Ragg, G. Fronza, G. Raos, V. Macon, *Angew. Chem.* **2006**, *118*, 1141–1144; *Angew. Chem. Int. Ed.* **2006**, *45*, 1123–1126; d) A. Mele, *Chim. Oggi/Chem. Today* **2010**, *28*, 48–53.
[4] a) *Ionic Liquids*, *Faraday Disc.*, *Vol. 154*, RSC Publishing, London, **2012**, pp. 454–457; b) H. Weingärtner, *Angew. Chem.* **2008**, *120*, 664–682; *Angew. Chem. Int. Ed.* **2008**, *47*, 654–670.
[5] C. Schröder, C. Wakai, H. Weingärtner, O. Steinhauser, *J. Chem. Phys.* **2007**, *126*, 084511.
[6] For experimental studies see: a) C. Daguenet, P. J. Dyson, I. Krossing, A. Oleinikova, J. Slattery, H. Weingärtner, *J. Phys. Chem. B* **2006**, *110*, 12682–12688; b) R. Buchner, G. Hefter, *Phys. Chem. Chem. Phys.* **2009**, *11*, 8984–8999. For MD simulations see: c) C. Schröder, M. Haberler, O. Steinhauser, *J. Chem. Phys.* **2008**, *128*, 134501; d) C. Schröder, O. Steinhauser, *J. Chem. Phys.* **2009**, *131*, 114504.
[7] K. Modig, E. Liepinsh, G. Otting, B. Halle, *J. Am. Chem. Soc.* **2004**, *126*, 102–114.
[8] B. Halle, *J. Chem. Phys.* **2003**, *119*, 12372–12385.

[9] S. Gabl, H. Weingärtner, O. Steinhauser, in preparation.
[10] L. Nordstierna, P. V. Yushmanov, I. Furo, *J. Chem. Phys.* **2006**, *125*, 074704.
[11] a) A. Abragam, *The Principles of Nuclear Magnetism*, Clarendon, Oxford, **1961**, chap. VIII, pp. 300 – 305; b) Y. Ayant, E. Belorizky, P. Fries, J. Rosset, *J. Phys. (Paris)* **1977**, *38*, 325 – 337; c) L.-P. Hwang, J. H. Fried, *J. Chem. Phys.* **1975**, *63*, 4017 – 4025; d) for a review of early theoretical and experimental work see: "Nuclear spin relaxation and intermolecular interactions": H. G. Hertz, A. Kratochwill, H. Weingärtner in *Stud. Phys. Theor. Chem.*, *Vol. 37* (Eds.: W. J. Orville-Thomas, H. Ratjczak, C. N. R. Rao), Elsevier, Amsterdam, **1985**, chap. 8.
[12] C. Schröder, O. Steinhauser, unpublished results.
[13] K. Hayamizu, S. Tsuzuki, S. Seki, Y. Umebayasi, *J. Phys. Chem. B* **2012**, *116*, 11284 – 11291.

